isvr Institute of Sound and Vibration Research

Theoretical Investigation of Wheel/Rail Non-linear Interaction due to Roughness Excitation

T.X. Wu and D.J. Thompson

ISVR Technical Memorandum 852

August 2000

University of Southampton

SCIENTIFIC PUBLICATIONS BY THE ISVR

Technical Reports are published to promote timely dissemination of research results by ISVR personnel. This medium permits more detailed presentation than is usually acceptable for scientific journals. Responsibility for both the content and any opinions expressed rests entirely with the author(s).

Technical Memoranda are produced to enable the early or preliminary release of information by ISVR personnel where such release is deemed to the appropriate. Information contained in these memoranda may be incomplete, or form part of a continuing programme; this should be borne in mind when using or quoting from these documents.

Contract Reports are produced to record the results of scientific work carried out for sponsors, under contract. The ISVR treats these reports as confidential to sponsors and does not make them available for general circulation. Individual sponsors may, however, authorize subsequent release of the material.

UNIVERSITY OF SOUTHAMPTON

INSTITUTE OF SOUND AND VIBRATION RESEARCH

DYNAMICS GROUP

Theoretical Investigation of Wheel/Rail Non-linear Interaction due to Roughness Excitation

by

T.X. Wu and D.J. Thompson

ISVR Technical Memorandum No. 852

August 2000

Authorized for issue by
Dr. M.J. Brennan
Group Chairman

TABLE OF CONTENTS

ABSTRACT

A study is presented of the non-linear dynamic interaction between a wheel and rail, excited by roughness on the wheel and rail contact surfaces. A moving irregularity model is used to represent the wheel/rail interaction process in the time-domain. A low order multiple degree-of-freedom system is developed to approximate the infinite track for numerical simulations. The effects of the non-linear contact on the wheel/rail dynamic interaction are investigated through calculations, analysis and comparisons with the results from a linear contact model. The difference between the non-linear and linear interactions is found to be small if the roughness level is not extremely severe and a typical static contact preload exists. The difference increases for low preloads or for high roughness amplitudes. For example, if the wheel and rail surfaces are in good condition (r.m.s. amplitudes of roughness below 15 μm), the linear model can be used without significant error for all static loads down to 25 kN (equivalent to an unloaded container wagon). When the track is corrugated with an r.m.s. amplitude of 25 μm, good agreement between linear and non-linear models is obtained for static loads of 50 kN and above, typical of passenger stock or loaded freight vehicles, but differences of up to 4 dB in one-third octave force levels are found at 25 kN. Differences between the linear and non-linear models are found to occur when the r.m.s. roughness amplitude is more than 0.35 times the static deflection of the contact zone; significant loss of contact occurs at amplitudes about 1.5 times greater than this.

1. INTRODUCTION

Small-scale unevenness on the wheel and rail contact surfaces, referred to as roughness, induces high frequency dynamic interaction between the wheel and rail when a train runs on the track. As a result, the wheel and rail are excited, vibrate and radiate noise. It is important to know the wheel/rail interaction force for predicting track and wheel vibration, railway noise radiation as well as the formation of wheel and rail corrugation or track damage.

Two main types of model have been used to study wheel/rail interactions. One represents a wheel (or wheels/vehicle) rolling over roughness on the rail. This model was used by Ripke [1], Sibaei [2] and Nielson and Igeland [3]. The other is a moving irregularity model. This model can be regarded as one in which the wheel remains in a fixed position on the rail, and a strip combining the roughness on the wheel tread and railhead is effectively pulled at a steady speed between wheel and rail. The combined roughness forms a relative displacement input between the wheel and rail, and thus the wheel/rail interaction force depends on the dynamic properties of the wheel and rail (including the contact zone) at the contact position. The moving irregularity model has been widely used to investigate problems of wheel/rail interaction and rolling noise, for example by Frýba [4], Remington [5] and Grassie et al. [6]. For high frequency vibration of railway track, for example above 50 Hz, the wave speed in the rail (hundreds of metres per second) is much higher than the train speed (tens of metres per second), and therefore assuming the wheel is stationary is an acceptable approximation which brings much convenience for studying wheel/rail interaction and vibration.

For a linear system which is not time-varying, the equation of motion can be expressed in the frequency-domain. In a simple case of vertical interaction between wheel and rail, the contact force F can be given as in [6]

$$F(\omega) = -\frac{R(\omega)}{\alpha^{W}(\omega) + \alpha^{C}(\omega) + \alpha^{R}(\omega)} \tag{1}$$

where R is the relative displacement (roughness) between the wheel and rail, α^W, α^C and α^R are the point receptances (displacement divided by force) of the wheel, contact spring and rail respectively and ω is the circular frequency of the excitation (roughness). This was extended by Thompson [7] to give a more comprehensive model, which can be used for calculating the wheel-rail dynamic interaction forces in six degrees of freedom.

The contact receptance, α^C, represents the local elastic deformation of the wheel and rail in their contact zone. In general, however, the contact stiffness between the wheel and rail is non-linear and can be approximated by the Hertz law [8], whereas equation (1) is derived based on the assumption of a linear contact spring. A non-linear contact stiffness, combined with linear wheel/vehicle and track models, was used by Newton and Clark *et al.* [9, 10], Nielson and Igeland [3, 11], Ripke [1] and Ilias [12]. The representation of a non-linear wheel/rail contact force is not complex mathematically, it being proportional to the contact deflection to the power 3/2. However, the superposition principle does not hold for a system containing a non-linear element and thus calculations in the time-domain are essential rather than in the frequency-domain. Although much work concerning track dynamics using a non-linear wheel/rail contact stiffness has been done as mentioned above, it is still not very clear to what extent the non-linear contact stiffness affects the wheel/rail interaction and thus the wheel and rail vibration, and how different the results could be from the linear and non-linear models in practice. Ripke [1], for example, found significant differences between linear and non-linear contact stiffness, but this was based on a constant roughness amplitude of ±25 μm at all frequencies which is rather large, especially at high frequencies. In addition, these models must be extended to considerably higher frequencies to allow them to predict noise radiation (at least 5 kHz instead of, typically, 1500 Hz).

The purpose of this study is to explore to what extent the wheel/rail interaction and the wheel and track vibration are affected by the non-linear contact stiffness, and thus to be able to indicate in which cases the non-linearity is important and where it is negligible. Firstly a non-linear wheel/track interaction model is introduced and an alternative multiple degree-of-freedom model (MDOF) representing an infinite track is developed. Based on the MDOF model, a simplified non-linear wheel/track interaction model in state-space form is set up for numerical simulations. Finally the non-linear interaction and the wheel and rail vibration are calculated, analysed and compared with the results from the linear contact model to examine the effects of the non-linear contact.

In this paper, only the vertical wheel/track elastic interaction is studied, as caused by the relative displacement excitation (roughness). Other factors such as the tangential contact and the creep force, are not considered here. Only the non-linearity in the contact zone is considered, not the non-linearity of the track support. The frequency range of interest is 50 to 5000 Hz.

2. SIMPLIFIED WHEEL/RAIL INTERACTION MODEL

2.1. WHEEL/RAIL INTERACTION MODEL

Figure 1 shows the form of the wheel/rail interaction. Here the moving irregularity model is used, in which a roughness is pulled between a stationary wheel and the rail. In this system there are three dynamic systems; the wheel and track are considered to be linear, while the contact stiffness is non-linear. For simplicity the wheel is represented by a mass (its unsprung mass). As only higher frequency vibration above 50 Hz is of interest here, the coupling with the vehicle vibration is ignored because it is isolated by the soft suspension springs.

The force-deflection relation of the contact stiffness is assumed to follow the Hertz law and can be given in the form

$$f = C_H (x_w - x_r - r)^{3/2} \tag{2}$$

where f is the wheel/rail contact force, x_w and x_r are the wheel and rail displacement respectively, r is the roughness and C_H is the Hertzian constant. This expression is exact for cylindrical surfaces, which meet at an elliptical contact patch, and provides an approximation for other contact geometry. The excitation, the roughness r, can be regarded as a broad band process from a practical point of view, for example, the roughness wavelengths of relevance for rolling noise are typically in the range 5 mm to 0.5 m. At a train speed of 100 km/h (27.8 m/s) these wavelengths correspond to a frequency range 55 – 5500 Hz, the shorter wavelengths applying to higher frequencies.

The track is the most complicated of the three sub-systems. Usually the vertical track dynamics can be described in this frequency range by an infinite Timoshenko beam with continuous or discrete spring-mass-spring supports representing railpad, sleeper and ballast, see reference [13]. However, such a model brings great difficulties in calculations of the wheel/rail interaction with non-linearity. To make the mathematical treatment easier, some simpler alternative models for track dynamics need to be developed. Before doing this, a concise introduction of the track dynamic behaviour is given.

2.2. INTRODUCTION OF TRACK DYNAMICS

Track models are used to calculate the rail vibration and to determine the wheel/rail interaction force. In terms of the wheel/rail vertical interaction up to about 5 kHz, cross-sectional deformations of the rail that occur at high frequencies are not important and thus the rail can be well approximated by a Timoshenko beam model. Two such models are commonly used [6, 13]: (a) an infinite rail continuously supported by damped resilient and mass layers (railpads, sleepers and ballast); (b) an infinite rail discretely supported by pad, sleeper and

ballast. Using a track model with discrete supports the so-called pinned-pinned resonance can be observed, in which the track receptance has a maximum when the excitation acts between sleepers and a minimum when the excitation acts at a sleeper. This occurs because the sleeper spacing is equal to half the wavelength of the flexural waves at this frequency. Apart from the pinned-pinned resonance, the two track models have a similar dynamic behaviour.

Figure 2 shows the point receptance of a typical track (displacement per unit force at the forcing point) from a continuous model and a discrete model with the force acting at mid-span between sleepers. The parameters for the track models are listed in Table 1. Three resonance peaks can be seen, at about 80 Hz, 520 Hz and 1050 Hz. At 80 Hz the whole track bounces on the vertical stiffness of the ballast, while at 520 Hz the rail vibrates on the pad stiffness, the latter frequency depending on the pad stiffness. The sharp peak at 1050 Hz is the pinned-pinned resonance, which can only be observed using a discretely supported track model. Detailed analysis of track dynamics can be found in references [14, 15] and an extensive review of literature by Knothe and Grassie [16].

2.3. EQUIVALENT MDOF TRACK MODEL

In order to allow for non-linear analysis of the wheel/rail interaction in the time-domain, an equivalent multiple degree-of-freedom (MDOF) model for track dynamics is needed to represent an infinite beam model. Nielson and Igeland [3] developed an MDOF model for a 22 m long track section using the finite element method. To reduce the scale of the problem, a modal synthesis technique was applied to the FE model (using only 185 modes).

Another possibility that can be considered is to approximate in a least-square sense a frequency response function (receptance) from an existing infinite track model by a limited modal decomposition. This approach was used by Fingberg [17]. A similar methodology is

used here to represent an infinite track model by an MDOF model that has approximately the same frequency response function as the infinite track.

Firstly the frequency response function (point receptance curve) of an infinite track to be approximated should be chosen. It is chosen here from the result of the continuously supported track model given in Figure 2. This is because the pinned-pinned resonance phenomenon, due to the infinite beam structure with periodic supports, has sharp peaks and troughs in both magnitude and phase which cannot be well fitted by an MDOF system. On the other hand, in practice it has been found that the pinned-pinned resonance may be cancelled or suppressed due to the wave reflections from other wheels or due to the random sleeper spacing [18, 19]. Therefore the receptance curve from the continuously supported track model can be used to take advantage of its simpler form which is more amenable to be approximated by an equivalent MDOF system.

The second step is to find an equivalent system corresponding to the point receptance of the infinite track. The system should have a transfer function expressed in the form of a ratio of two polynomials, so that conventional system theory can be applied for setting up a mathematical model in the time-domain. This is actually a curve fitting problem for which the function 'invfreqs' in the Signal Processing Toolbox of MATLAB has been used. This function returns the real numerator and denominator coefficient vectors b and a of the transfer function

$$H(s) = \frac{B(s)}{A(s)} = \frac{b_1 s^m + b_2 s^{m-1} + \ldots + b_{m+1}}{s^n + a_1 s^{n-1} + \ldots + a_n} \tag{3}$$

whose complex frequency response approximates the required frequency response at specified frequency points. Scalars m and n specify the desired orders of the numerator and denominator polynomials. More details about the algorithm of this function can be found in [20]. The most important point for using this function is that whatever values of m and n are selected, it must

be ensured that all the poles of the returned transfer function $H(s)$ are in the left half-plane and thus the system is stable. From considerable experimentation it has been found that high order systems cannot bring better results than a low order one. Figure 3 shows the frequency response $H(\omega)$ which is obtained by choosing $m = 3$ and $n = 4$ to approximate the point receptance of the continuously supported track. The values of b_i and a_i for the numerator and denominator polynomials are listed in Table 2.

The point receptance of the infinite track model is also shown in Figure 3 for comparison. It can be seen that $H(\omega)$ is in good agreement with the point receptance of the infinite track model in the whole frequency region 50 – 5000 Hz.

Finally a mathematical model in the time-domain needs to be set up in accordance with the transfer function $H(s)$. An equivalent differential equation corresponding to $H(s)$ (m = 3 and n = 4) can be given as

$$(D^4 + a_1 D^3 + a_2 D^2 + a_3 D + a_4)\, y(t) = (b_1 D^3 + b_2 D^2 + b_3 D + b_4)\, f(t) \tag{4}$$

where D represents differential operator d/dt. $y(t)$ and $f(t)$ are the output and input of the system and in relation to the track vibration they represent the rail displacement and wheel/rail interaction force respectively. The state-space representation of equation (4) can be expressed as follows (see reference [21]):

$$\begin{bmatrix} \dot{x}_1 \\ \dot{x}_2 \\ \dot{x}_3 \\ \dot{x}_4 \end{bmatrix} = \begin{bmatrix} -a_1 & 1 & 0 & 0 \\ -a_2 & 0 & 1 & 0 \\ -a_3 & 0 & 0 & 1 \\ -a_4 & 0 & 0 & 0 \end{bmatrix} \begin{bmatrix} x_1 \\ x_2 \\ x_3 \\ x_4 \end{bmatrix} + \begin{bmatrix} b_1 \\ b_2 \\ b_3 \\ b_4 \end{bmatrix} f(t) \tag{5}$$

$$y(t) = x_1(t) \tag{6}$$

In equation (5) only f and x_1 have explicit physical meanings and represent the force and displacement at the forcing point respectively. The others have no direct physical meanings.

Nevertheless the system described by equation (5) has a similar frequency response function to that of an infinite track and thus is an alternative representation for the track model.

2.4. EQUATION OF WHEEL/RAIL INTERACTION

Referring to Figure 1, the equation of motion for the wheel/rail interaction and the wheel and rail vibration can be written as follows, using the equivalent MDOF model for the track dynamics:

$$\begin{bmatrix} \dot{x}_1 \\ \dot{x}_2 \\ \dot{x}_3 \\ \dot{x}_4 \end{bmatrix} = \begin{bmatrix} -a_1 & 1 & 0 & 0 \\ -a_2 & 0 & 1 & 0 \\ -a_3 & 0 & 0 & 1 \\ -a_4 & 0 & 0 & 0 \end{bmatrix} \begin{bmatrix} x_1 \\ x_2 \\ x_3 \\ x_4 \end{bmatrix} + \begin{bmatrix} b_1 \\ b_2 \\ b_3 \\ b_4 \end{bmatrix} f \tag{7a}$$

$$\begin{aligned} \dot{x}_5 &= x_6 \\ \dot{x}_6 &= (W - f)/M_w \end{aligned} \tag{7b}$$

$$f = \begin{cases} C_H (x_5 - x_1 - r)^{3/2}, & x_5 - x_1 - r > 0 \\ 0, & x_5 - x_1 - r \le 0 \end{cases} \tag{7c}$$

where $x_5 = x_w$ is the wheel displacement, $x_1 = x_r$ is the rail displacement, W is the static load at one wheel from the weight of the vehicle, M_w is the wheel mass (unsprung mass), f is the non-linear wheel/rail interaction force, C_H is the Hertzian constant and r is the roughness excitation. Equations (7) can be solved numerically using the Runge-Kutta method.

3. WHEEL/RAIL INTERACTION DUE TO A HARMONIC ROUGHNESS

3.1. CASES CONSIDERED

In this section the wheel/rail interaction and vibration are investigated using a single harmonic roughness input at various frequency points in the region 50 – 5000 Hz. In this way the effects on the wheel/rail interaction of the non-linear contact can be examined at each frequency considered. This is useful because the wheel/rail interaction is

determined by the dynamic response of three components: the wheel, track and contact spring. The frequency response functions of the wheel and track have significant influences on the wheel/rail interaction (refer to equation (1)). These influences need to be studied first for a better understanding of the non-linear wheel/rail interaction. Since the superposition principle does not hold for non-linear systems, the responses predicted here do not represent spectra due to broad band roughness, rather they are the response to single frequency roughness at a range of frequencies.

Typically, roughness levels are found to be high for long wavelength roughness (causing low frequency excitation) and low for short wavelengths (causing high frequency excitation), see reference [22]. For simplicity the magnitude of the roughness is assumed here to be inversely proportional to the frequency at which the roughness is applied as an excitation to the wheel, rail and contact spring system, as shown in Figure 4. Thus, for example, at 1000 Hz the roughness amplitude is taken as ±10 μm. The parameters of the system are listed in Table 1.

In practice, wheel loads vary over a wide range; an unloaded bogie container wagon for example has a wheel load of about 25 kN, unloaded light rail and metro passenger vehicles are typically 35-40 kN, mainline passenger vehicles range from about 40 to 60 kN, while loaded freight vehicles have wheel loads in excess of 100 kN. Two static load situations are considered in the calculations in this section, W = 25 kN and 50 kN, representing an unloaded container wagon and a typical passenger vehicle respectively. For comparison the equivalent linear contact stiffness cases are also calculated. The tangent stiffness, $K_t = df/du$, with u the contact deflection, is used in the linear model and is chosen according to the static load applied.

3.2. NUMERICAL RESULTS

The fourth order Runge-Kutta method is used for numerical simulations of equations (7). Figure 5(a) shows the general results in terms of maximum wheel/rail dynamic interaction force, for frequencies in the region 50 – 5000 Hz, due to the roughness excitation amplitude shown in Figure 4. This maximum dynamic force is obtained by subtracting the static load from the peak contact force. The results from equivalent linear cases (using equation (1)) are also presented in Figure 5(a).

The interaction force can be seen to vary with frequency in a manner which follows the inverse of the track receptance (Figure 3) for frequencies up to 900 Hz. Compared with the linear case, the non-linear effects due to the roughness input shown in Figure 4 are only noticeable in the frequency region around 200 Hz and 900 Hz and only for the lighter static load. The ratio of the non-linear wheel/rail interaction force to the linear one is shown in Figure 5(b). This shows that the greatest difference between the two cases is only five percent. Slight loss of contact between the wheel and rail occurs for excitation at about 200 – 250 Hz, but it does not affect the magnitude of the interaction force greatly.

A larger roughness input is also considered of three times that given in Figure 4. In this case the non-linear effects are significant, as seen in Figure 5(b), because of severe loss of contact between the wheel and rail. Loss of contact occurs for excitation at low frequencies up to 70 Hz and from 150 to 300 Hz due to the very large roughness amplitudes.

Figures 6 – 8 show examples of the non-linear contact forces and the vibrations of the wheel and track in the time-domain at 180 Hz, 1 kHz and 3 kHz respectively. These results are for an arbitrary time period once steady state has been reached in each case. From Figure 6(a), compared with the linear interaction, the effects of the non-linearity at 180 Hz can be identified. The half-period when the contact force is greater than the static load can be

observed to be slightly shorter than the other half-period in which the contact force is below the static load. Thus some super-harmonic components are generated in the responses of the system, although their magnitudes are very small. This is shown in Figure 6(b). For example the component at 360 Hz has an amplitude of about 5% of the 180 Hz component.

Comparing the three cases in Figures 6 – 8, both the wheel and the rail responses are large at 180 Hz, whereas the wheel response is very small at 1 kHz and the rail response is also small at 3 kHz. Moreover the wheel is almost stationary at 3 kHz. The wheel/rail interaction is therefore determined by the contact spring, wheel and track at 180 Hz, by the contact spring and track at 1 kHz and by the contact spring alone at 3 kHz.

3.3. ANALYSIS OF THE NON-LINEAR EFFECTS

Although the effects of non-linearity are found to be limited according to the numerical simulations when the roughness input is not large, a detailed analysis of how the non-linear contact affects the wheel/rail interaction is helpful. The analysis here is carried out both from aspects of the non-linearity of the contact stiffness and the dynamic properties of the wheel and track.

Figure 9(a) shows the force-deflection curve of the non-linear contact spring. Using Taylor series the non-linear contact force-deflection relation can be written as

$$f(u) = f(u_0) + \frac{df(u_0)}{du}(u-u_0) + \frac{d^2 f(u_0)}{du^2}\frac{(u-u_0)^2}{2!} + \cdots\cdots \tag{8}$$

where u is the contact deflection and u_0 is the deflection under a certain static load. Thus $f(u_0)$ represents the static load W and $df(u_0)/du$ is the tangent stiffness K_t under this static load. Two tangents are shown in Figure 9(a) at the load points W = 25 kN and 50 kN. They are equal to the first two terms (linear terms) from the right-hand side in equation (8) and represent the equivalent linear contact stiffness under the load considered. The differences

between the linear and non-linear contact can be observed in Figure 9(b) in terms of the ratio of the non-linear contact force to the linear one. For a given deflection, the non-linear contact force can be seen to be closer to the linear one if a greater static load is applied. Thus it is clear that the influence of the non-linear contact is weaker when the static load is greater. This is observed in the results of Figure 5(b).

In addition the deviations between the non-linear and linear contact forces in Figure 9(b) increase with increasing contact deflection. The magnitude of the contact deflection is determined by both the roughness level and the dynamic behaviour of the wheel and track. Therefore it can be expected that the extent of non-linear effects is also affected by the dynamic properties of the wheel and track.

Figure 10(a) shows the receptances of the wheel, track and the equivalent tangent contact stiffness under the static load of 25 kN and 50 kN in the frequency region 50 – 5000 Hz. Figure 10(b) indicates the ratio of the dynamic contact deflection to the roughness input. It can be seen from Figure 10(a) that the wheel and track receptances are much greater than that of the contact stiffness at low frequencies so that the contact spring here can be regarded as effectively rigid. Because of this the ratio of the contact deflection to the roughness (Figure 10(b)) is very small at low frequencies. Thus the large roughness input at low frequencies only results in small contact deflection. The wheel/rail interactions therefore are almost the same whether they are based on the linear or non-linear model as long as loss of contact does not occur. If severe loss of contact occurs due to a very large roughness input, however, the non-linear contact force is larger than the linear one since the non-linear contact spring becomes stiffer with increasing deflection. Such results are found in Figure 5(b).

Around 200 Hz and 900 Hz the receptances of the wheel, track and contact spring are similar in magnitude. Moreover, around 200 Hz the roughness level is still high and the ratio of the contact deflection to the roughness rises to about 0.6, whilst around 900 Hz this ratio is

close to 1, although the roughness level assumed here is not as high as at 200 Hz. As a result, in both cases the contact deflection is relatively large and the non-linear contact becomes important. This explains why the non-linear effects are most noticeable around 200 Hz and, to a lesser extent, 900 Hz in Figure 5.

As both the wheel and the track receptances are much smaller than that of the contact spring at high frequencies, the contact deflection is virtually equal to the roughness above 1 kHz. This might suggest that the non-linear contact would now dominate. On the other hand, however, the roughness magnitude at short wavelength is fairly low in practice. As a result, the effects of the non-linearity are very limited because of the small dynamic contact deflection. As the ratio of the contact deflection to the roughness input is quite stable above 1 kHz and slightly higher than 1, the effects of non-linear contact are here determined purely by the roughness magnitude for a given static contact load.

The above analysis is based on the condition that no loss of contact occurs between the wheel and rail. When loss of contact occurs due to large roughness input, the difference in the contact forces between linear and non-linear models can be large, as shown in Figure 5(b). This is because the wheel and rail are bound to remain in contact in the linear model.

4. WHEEL/RAIL INTERACTION DUE TO A BROAD BAND RANDOM ROUGHNESS

4.1. RANDOM ROUGHNESS INPUT

So far, sinusoidal roughness at different frequencies has been considered. In practice, the roughness excitation is composed of unevenness on the wheel and rail contact surfaces having a broad band spectrum over a range of wavelengths. When a train runs on the rails, the unevenness forms an excitation with multiple frequency components which can be regarded as a broad band random process. On the other hand, since a non-linear contact stiffness is taken account of in the wheel/rail interaction model, the superposition principle does not hold here

and frequency-domain analysis according to equation (1) cannot be performed. A practical roughness input is therefore needed to simulate the wheel/rail interaction and the responses of the wheel and track in the time-domain.

Figure 11 shows four one-third octave band roughness spectra. The solid line corresponds to the roughness of a wheel with cast-iron block brakes on good quality track at 100 km/h, while the dotted line corresponds to corrugated track at 140 km/h [23]. Two other spectra are also shown: an intermediate roughness which is the geometric mean of the above two spectra, and an extreme roughness which has twice the amplitude of the corrugated rail spectrum. Summing these spectra for the frequency bands 250 Hz and above, the r.m.s. amplitudes of the roughness are found to be 7.6, 13.2, 25 and 50 μm.

Starting from each of these spectra, a narrow-band spectrum is generated, with a bandwidth of 5 Hz, which corresponds to the one-third octave band spectrum. For simplicity, this contains equal energy in each narrow band within a given 1/3 octave band. Below 50 Hz the magnitude of the spectrum is set to 0.

This narrow-band spectrum is then used to generate a time series by using the inverse Fourier transform, the phase of each Fourier component being chosen randomly between $-\pi$ and π. This time series is used as the roughness input to the wheel/rail system.

4.2. RESULTS FOR RANDOM ROUGHNESS EXCITATION

Numerical simulations are carried out using equation (7) and a random roughness input which is constructed as described above. Results for the corrugated track roughness are presented in Figure 12, in terms of the non-linear contact force, contact deflection and displacements of the wheel and rail in the time-domain. The roughness input is also shown. The static load W here is chosen as 25 kN, corresponding to unloaded container wagons.

From Figure 12 the variations in the wheel/rail contact force can be seen to be very sharp. A sharp peak of the contact force appears when a sharp negative roughness input is applied. (The sign convention adopted for roughness is positive for a dip, negative for an asperity.) Some peaks in the contact force are as great as three times the static load, but complete unloading is rare. The wheel and rail displacements generally follow the roughness input, although the wheel cannot follow the high frequency components of the input due to its large inertia. Loss of contact or sharp peaks of the contact force are induced at large roughness dips or asperities. It can be observed from Figure 12 that the low frequency components in the rail response are delayed compared with the roughness input, whereas the high frequency components are out of phase with the input.

Because of the wheel and rail response properties, the dynamic contact deflection in Figure 12 can be seen to be much smaller than the roughness input and to consist mainly of high frequency components. As a result, the effects of the non-linear contact stiffness are not expected to be very noticeable provided loss of contact does not occur.

Figure 13 shows one-third octave band spectra of the wheel/rail dynamic interaction forces, from both the linear and the non-linear models, for the corrugated track and for a range of wheel static loads.

For the higher static loads, only small differences between the two models are found. For small values of load the contact force spectra decrease. The results from the non-linear model decrease more than those from the linear model around 250 and 800 Hz and do not appear to decrease for frequencies above 2 kHz. For a 50 kN static load, typical of passenger vehicles, it is found that non-linear interactions modify the force spectrum by at most 2 dB (in the 2 kHz band); for a 25 kN static load this maximum difference increases to 4 dB. Note that the preloads less than 25 kN are included to demonstrate the trends although they are unrealistically small for most situations.

Figure 14 shows the difference between the interaction force spectra predicted using non-linear and linear models for each load case. As well as the results for the corrugated track roughness shown in Figure 13, this also shows results for the other roughness spectra of Figure 11.

For the smoothest situation considered, the differences are all less than 0.5 dB, indicating that a linear model is adequate for this case. At the intermediate level of roughness, the linear model only gives significantly different results from the non-linear model for the lowest static load considered (10 kN), which is much less than normal values. As the roughness amplitude increases, however, the inadequacy of the linear model also becomes apparent at higher values of static load, as might be expected from the results of the previous section. Thus for the corrugated rail roughness the non-linear model is required for wheel loads of up to 35 kN, and for the extreme roughness for loads up to 70 kN.

In order to summarise these results, the mean is formed over all one-third octave frequency bands from 50 to 5000 Hz of the absolute differences in level given in Figure 14. This gives a single measure of the deviation between linear and non-linear models for the seven wheel loads and four roughness spectra considered. These results are plotted in Figure 15(a) against the ratio of the r.m.s. roughness amplitude (for 250 Hz and above) to the static deflection in the contact zone, u_0. The results for the four roughness spectra follow a similar trend. These results indicate that the difference between linear and non-linear models is negligible where the r.m.s. roughness amplitude is less than about 0.35 times the static contact deflection, and rapidly becomes significant above this.

In Figure 15(b) the percentage of the time that the wheel loses contact with the rail is plotted for each of the simulations. At low roughness no loss of contact occurs; the loss of contact rises to as much as 60% of the time for the extreme roughness spectrum and 10 kN load. These curves show similar trends to the deviations between linear and non-linear models

in Figure 15(a). However, it is found that loss of contact is only significant for r.m.s. roughness amplitudes above about 0.5 times the static contact deflection. Thus non-linear effects become important slightly before significant loss of contact occurs.

5. CONCLUSIONS

The effects of the non-linear contact on the wheel/rail dynamic interaction have been investigated through numerical simulations, analysis and comparisons with the results from the linear contact model. A simplified MDOF model equivalent to an infinite track has been developed, which has approximately the same frequency response function as the infinite track in the frequency region 50 – 5000 Hz. Using this equivalent track model a non-linear wheel/rail interaction model has been set up in state-space form for numerical simulations. The wheel/rail interaction has been investigated using both a single harmonic roughness excitation and a broad band random roughness input. The results are compared with those from the linear contact to check the effects of the non-linear contact. These effects are also analysed from the aspects of the non-linear contact force-deflection relationship and the dynamic behaviour of the wheel and track.

It has been found that the effects of the non-linear contact on the wheel/rail interaction are affected by the static preload and the dynamic properties of the wheel and rail. Under a large static contact load the non-linear effects on the wheel/rail dynamic interaction and vibration are weak and can be ignored. This is because the difference between the non-linear stiffness and the equivalent linear (tangent) stiffness is very small for a large static preload. The non-linear effects on the wheel/rail interaction are also not noticeable at low frequencies up to 100 Hz because in this frequency region the wheel and rail dynamic stiffness is much less than the contact stiffness and thus the latter can be regarded as effectively rigid, so that the question of its linearity is unimportant here. From a practical point of view, the non-linear effects are also

not noticeable at high frequencies (above 1 kHz) because the roughness level at short wavelengths is generally very low. In such a case the dynamic contact deflection is small and the non-linear contact force-deflection relation can be well approximated by a linear one. The non-linear effects are only noticeable when the roughness excitation is in the frequency region around 200 Hz and 900 Hz, where the dynamic stiffness of the wheel and rail is similar to the contact stiffness, but even so the difference between the non-linear and linear interactions is very limited.

The difference is also small when a typical broad band random roughness excitation is applied. In the examples considered, if the wheel and rail surfaces are in good condition (r.m.s. amplitudes of roughness below 15 μm), the linear model can be used without significant error for all static loads down to 25 kN (equivalent to an unloaded container wagon). When the track is corrugated with an r.m.s. amplitude of 25 μm, good agreement between linear and non-linear models is obtained for static loads of 50 kN and above, but agreement is less good for lower loads. Non-linear interactions modify the force spectrum by at most 2 dB for 50 kN; for 25 kN this increases to 4 dB.

When loss of contact occurs due to large roughness and lighter static load, the differences between linear and non-linear models become more significant. This is because the wheel and rail are bound to remain in contact in the linear model. In fact differences between the linear and non-linear models occur at slightly lower roughness amplitudes than those which induce significant loss of contact.

All the above suggests that the non-linear wheel/rail dynamic interaction model can be well approximated using an equivalent linear model when the roughness level is not extremely severe and a moderate static preload is applied to keep the wheel and rail in contact. Since a linear model can be expressed in the frequency domain, use of such a model greatly simplifies calculations.

ACKNOWLEDGEMENTS

The work described has been performed within the project 'Non-linear Effects at the Wheel/rail Interface and their Influence on Noise Generation' funded by EPSRC (Engineering and Physical Sciences Research Council of the United Kingdom), grant GR/M82455.

REFERENCES

1. B. Ripke 1995 *Fortschritt-Berichte VDI* Reihe 12, Nr. 249. Hochfrequente Gleismodellierung und Simulation der Fahrzeug-Gleis-Dynamik unter Verwendung einer nichtlienearen Kontaktmechanik.
2. Z. Sibaei 1992 *Fortschritt-Berichte VDI* Reihe 11, Nr. 165. Vertikale Gleisdynamik beim Abrollen eines Radsatzes - Behandlung im Frequenzbereich.
3. J. C. O. Nielson and A. Igeland 1995 *Journal of Sound and Vibration* 187, 825-839. Vertical dynamic interaction between train and track—influence of wheel and track imperfections.
4. L. Frýba 1988 *ILR-Bericht* **58**, 9-38. Dynamics of rail and track.
5. P. J. Remington 1987 *J. Acoust. Soc. Am.* **81**, 1805-1823. Wheel/rail rolling noise I: theoretical analysis.
6. S. L. Grassie, R. W. Gregory, D. Harrison and K. L. Johnson 1982 *Journal Mechanical Engineering Science* **24**, 77-90. The dynamic response of railway track to high frequency vertical excitation.
7. D. J. Thompson 1993 *Journal of Sound and Vibration* **161**, 387-400. Wheel-rail noise generation, part I: introduction and interaction model.
8. H. Hertz 1882 *Journal für die rein und angewandte Mathematik* **92**, 156-171. Über die Berührung fester elastischer Körper.
9. S. G. Newton and R. A. Clark 1979 *Journal Mechanical Engineering Science* **21**, 287-297. An investigation into the dynamic effects on the track of wheelflats on railway vehicles.
10. R. A. Clark, P. A. Dean, J. A. Elkins and S. G. Newton 1982 *Journal Mechanical Engineering Science* **24**, 65-76. An investigation into dynamic effects of railway vehicles running on corrugated rails.

11. A. Igeland 1996 *Proc. Instn. Mech. Engrs.* Part F **210**, 11-20. Railhead corrugation growth explained by dynamic interaction between track and bogie wheelsets.

12. H. Ilias and K. Knothe 1992 *Fortschritt-Berichte VDI* Reihe 12, Nr. 177. Ein diskret-kontinuierliches Gleismodell unter dem Einfluß schnell bewegter, harmonisch schwankener Wanderlasten.

13. D. J. Thompson and N. Vincent 1995 *Vehicle System Dynamics* Supplement **24**, 86-99. Track dynamic behaviour at high frequencies. Part 1: Theoretical models and laboratory measurements.

14. T. X. Wu and D. J. Thompson 1999 *Journal of Sound and Vibration* **224**, 329-348. A double Timoshenko beam model for vertical vibration analysis of railway track at high frequencies.

15. N. Vincent and D. J. Thompson 1995 *Vehicle System Dynamics* Supplement **24**, 100-114. Track dynamic behaviour at high frequencies. Part 2: Experimental results and comparisons with theory.

16. KL. Knothe and S. L. Grassie 1993 *Vehicle System Dynamics* **22**, 209-262. Modelling of railway track and vehicle/track interaction at high frequencies.

17. U. Fingberg 1990 *Journal of Sound and Vibration* **143**, 365-377. A model of wheel-rail squealing noise.

18. T. X. Wu and D. J. Thompson 2000 *Acta Acustica* **86**, (in press). The influence of random sleeper spacing and ballast stiffness on the vibration behaviour of railway track.

19. T. X. Wu and D. J. Thompson 1999 *Proceedings of Sixth International Congress on Sound and Vibration*, Lyngby, Denmark, 2629-2636. Effects of multiple wheels on a rail on the rail vibration.

20. T. P. Krauss, L. Shure and J. N. Little 1994 *Signal Processing Toolbox User's Guide*. The Math Works Inc.

21. F. H. Raven 1978 *Automatic Control Engineering*. Tokyo: McGraw-Hill; third edition.

22. D. J. Thompson 1996 *Journal of Sound and Vibration* **193**, 149-160. On the relationship between wheel and rail surface roughness and rolling noise.

23. P.C. Dings, M.G. Dittrich 1996 *Journal of Sound and Vibration* **193**, 103-112. Roughness on Dutch railway wheels and rails.

TABLE 1

Parameters of wheel and track

Wheel mass (all unsprung mass), kg	M_w	600
Hertzian constant, $N/m^{2/3}$	C_H	9.37×10^{10}
Young's modulus of rail, N/m^2	E	2.1×10^{11}
Shear modulus of rail, N/m^2	G	0.77×10^{11}
Density of rail, kg/m^3	ρ	7850
Loss factor of rail	η_r	0.01
Cross-section area of rail, m^2	A	7.69×10^{-3}
Area moment of inertia, m^4	I	30.55×10^{-6}
Shear coefficient	κ	0.4
Pad stiffness, N/m^2	k_p	5.83×10^{8}
Pad loss factor	η_p	0.25
Sleeper mass (half), kg/m	m_s	270
Ballast stiffness, N/m^2	k_b	8.33×10^{7}
Ballast loss factor	η_b	1
Distance between sleepers, m	d	0.6

TABLE 2

Parameters of MDOF track model

a_1	1.77×10^3	b_1	3.28×10^{-6}
a_2	1.26×10^7	b_2	1.87×10^{-2}
a_3	7.87×10^9	b_3	23.6
a_4	3.93×10^{12}	b_4	3.97×10^4

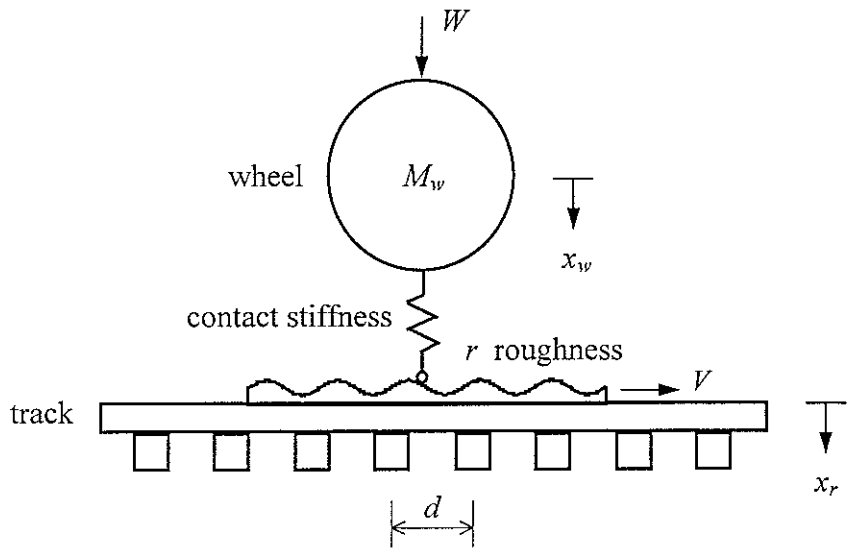

Figure 1. The moving irregularity wheel/rail interaction model, where V is the train speed.

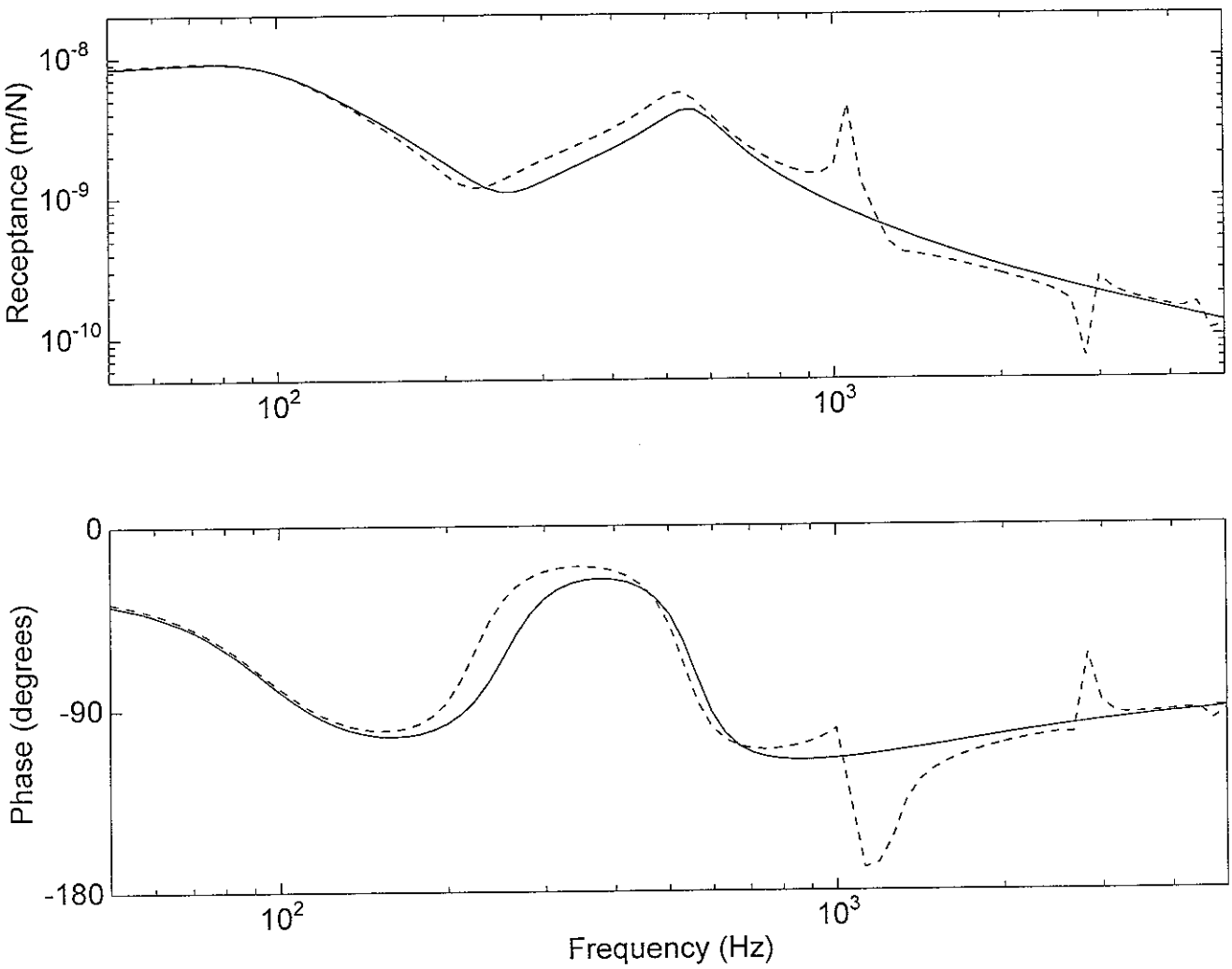

Figure 2. Magnitude and phase of the point receptance of an infinite track. — from the continuously supported track model, ····· from the discretely supported track model with force at mid-span.

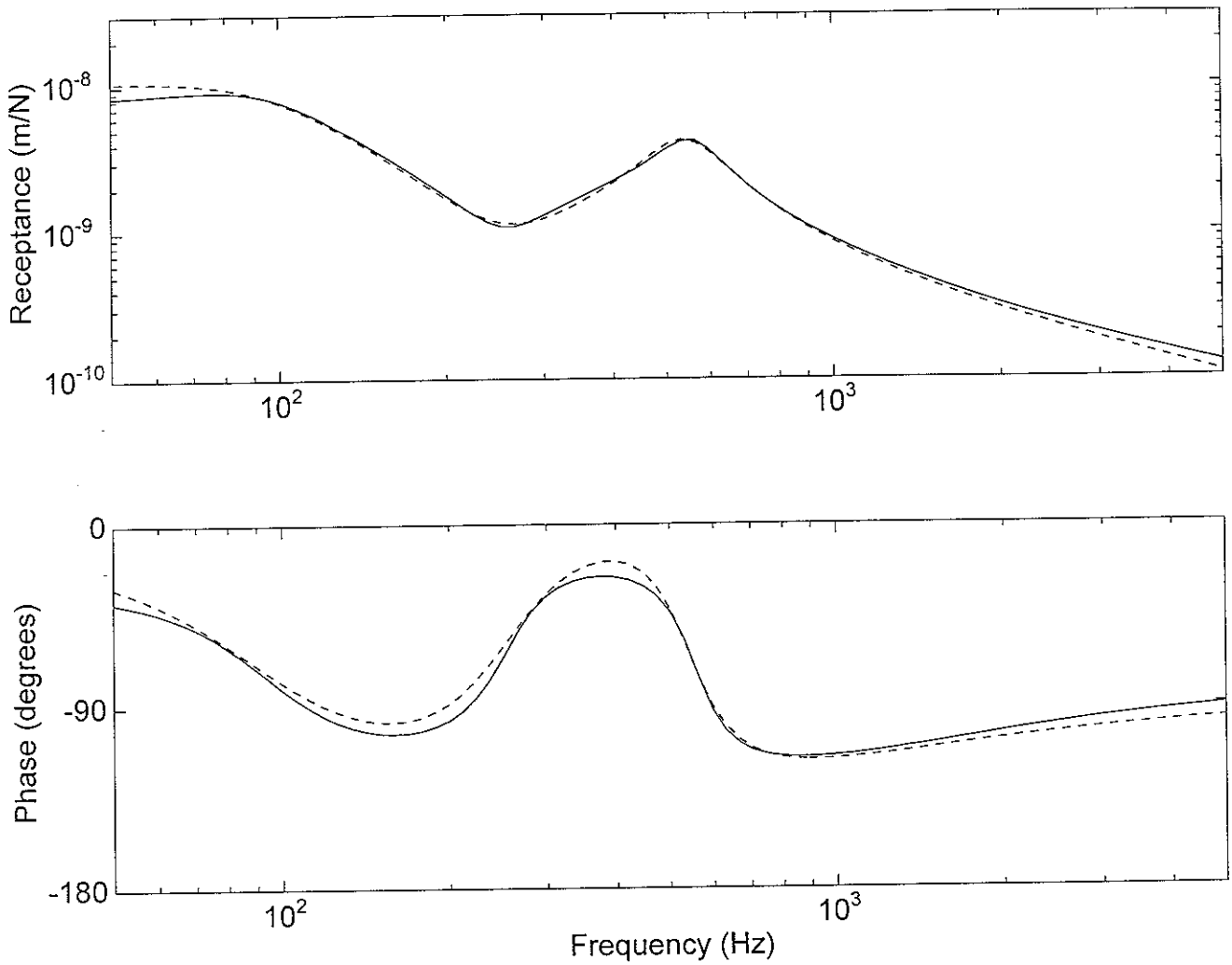

Figure 3. Magnitude and phase of the frequency response function. — from the infinite continuously supported track, ····· from the equivalent MDOF model.

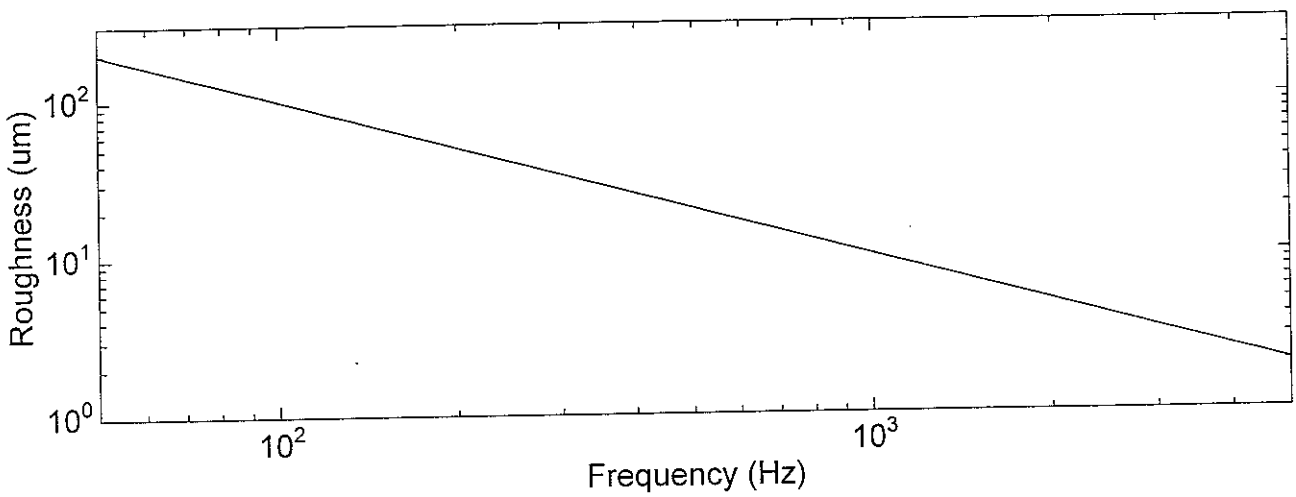

Figure 4. Assumed roughness amplitude for single frequency excitation.

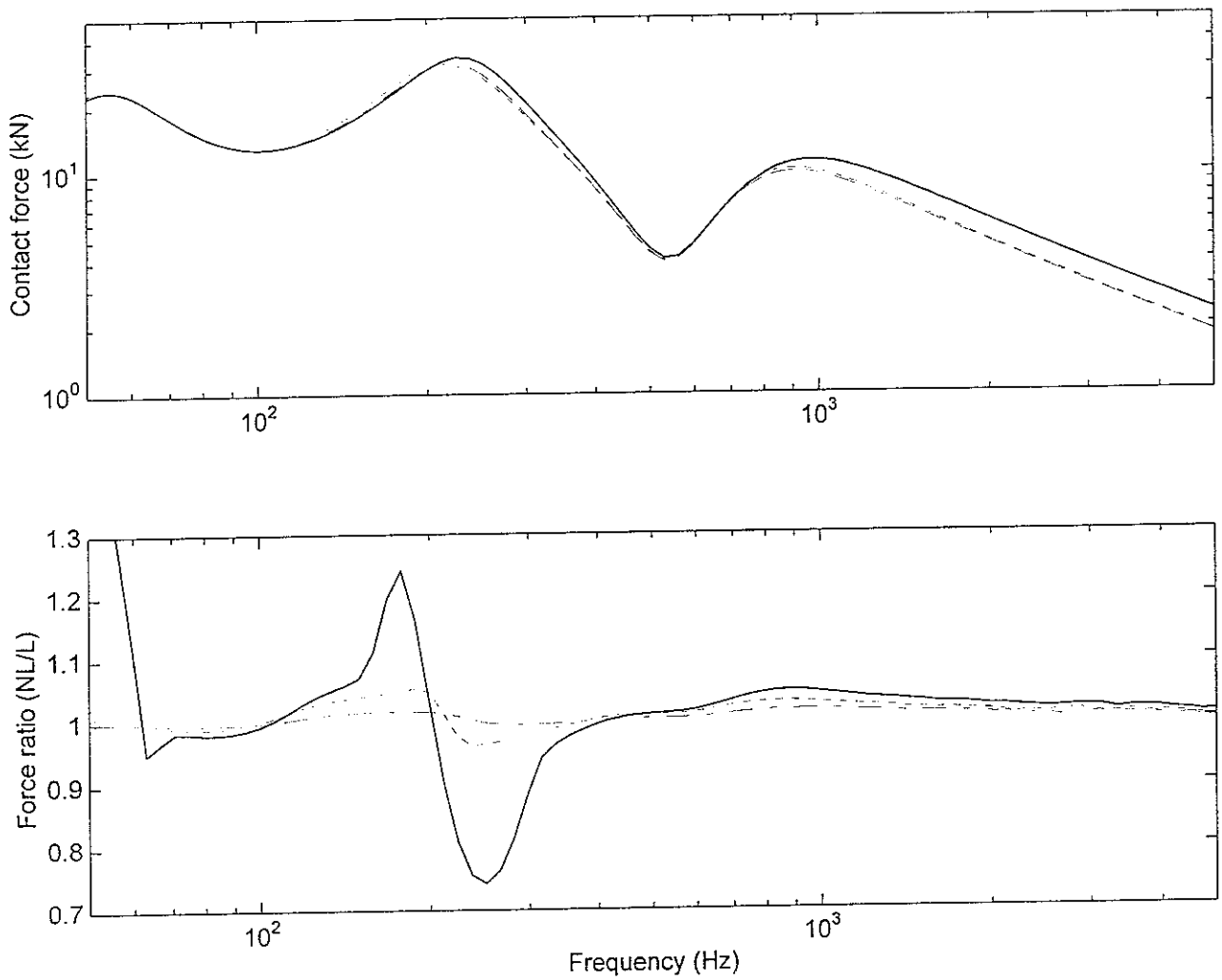

Figure 5. Maximum wheel/rail dynamic interaction force and the ratio of the non-linear to the linear interaction force. For the interaction force curves: — from the linear contact and the static load W = 50 kN, -·-·- from the non-linear contact, W = 50 kN, - - - from the linear contact, W = 25 kN, ····· from the non-linear contact, W = 25 kN. For the force ratio curves: -·-·- W = 50 kN, ····· W = 25 kN, — W = 50 kN, but the roughness amplitude is three times as high as that in Figure 4.

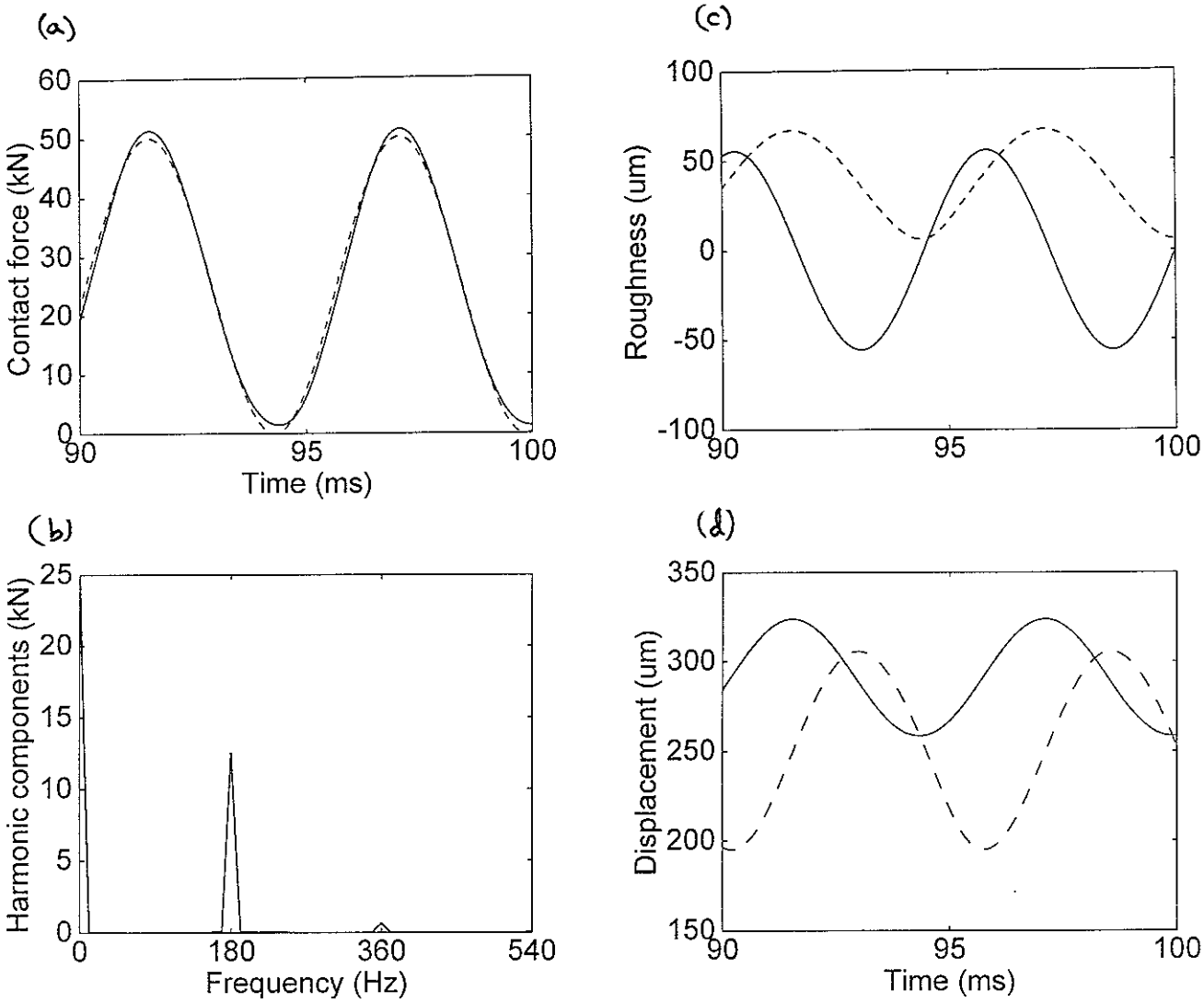

Figure 6. Wheel/rail interaction results for a static load $W = 25$ kN and excitation at 180 Hz. (a) The non-linear and linear wheel/rail contact forces, — from the non-linear contact, ····· from the linear contact, (b) frequency components of the non-linear contact force, (c) — roughness input, ····· contact deflection, (d) — wheel displacement, - - - rail displacement.

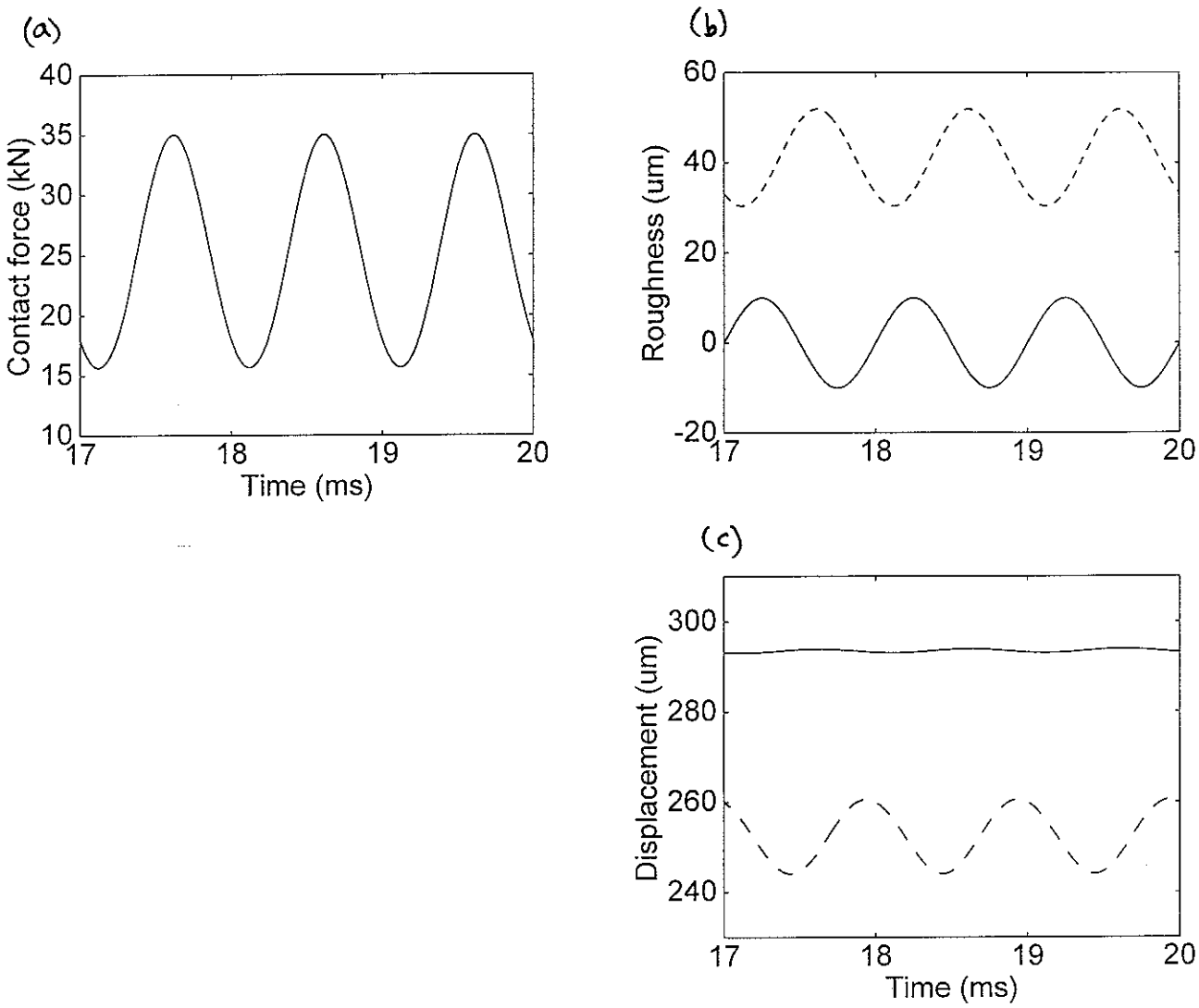

Figure 7. Results for a static load $W = 25$ kN and the excitation at 1 kHz. (a) The non-linear and linear wheel/rail contact forces, — from the non-linear contact, ····· from the linear contact, (b) — roughness input, ····· contact deflection, (c) — wheel displacement, - - - rail displacement.

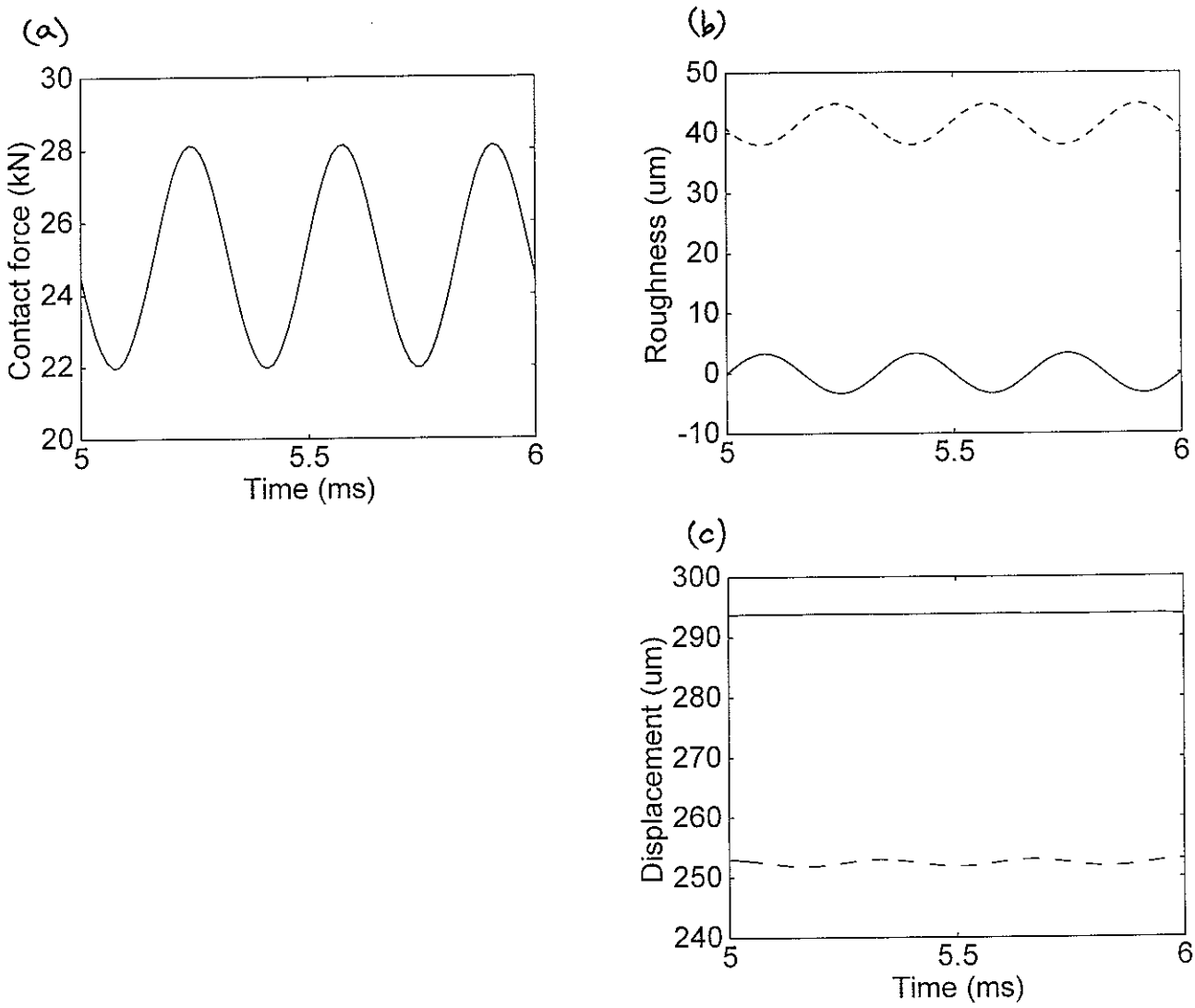

Figure 8. Results for a static load $W = 25$ kN and the excitation at 3 kHz. (a) The non-linear and linear wheel/rail contact forces, — from the non-linear contact, ····· from the linear contact, (b) — roughness input, ····· contact deflection, (c) — wheel displacement, - - - rail displacement.

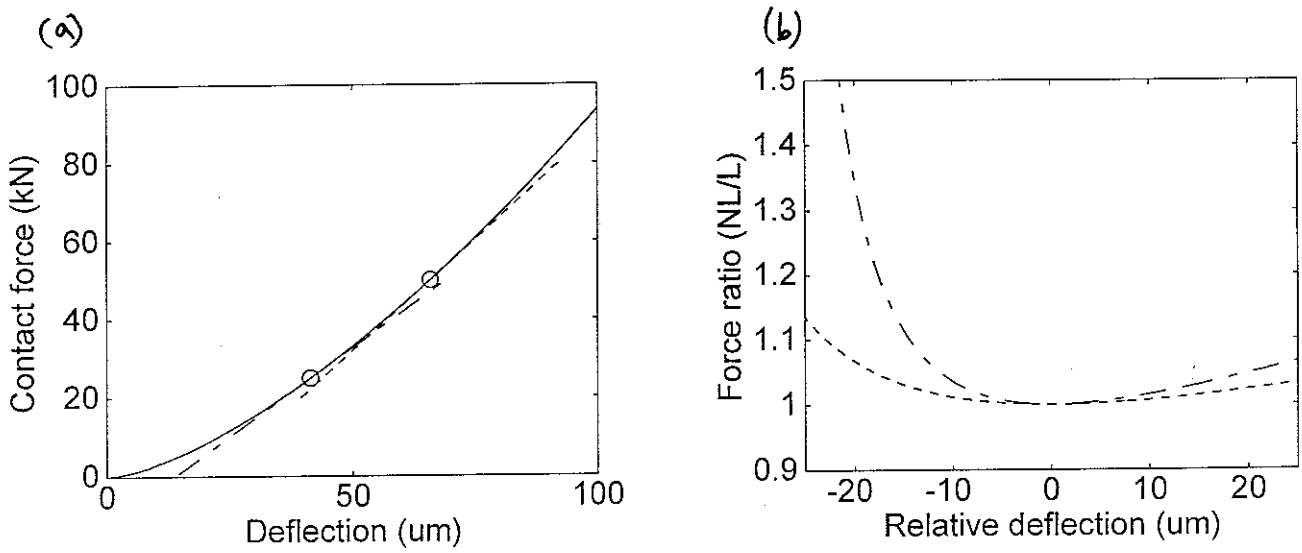

Figure 9. (a) Non-linear contact force-deflection relation, (b) ratios of the non-linear contact force to the equivalent linear contact force. ----- the static load $W = 25$ kN, ····· the static load $W = 50$ kN.

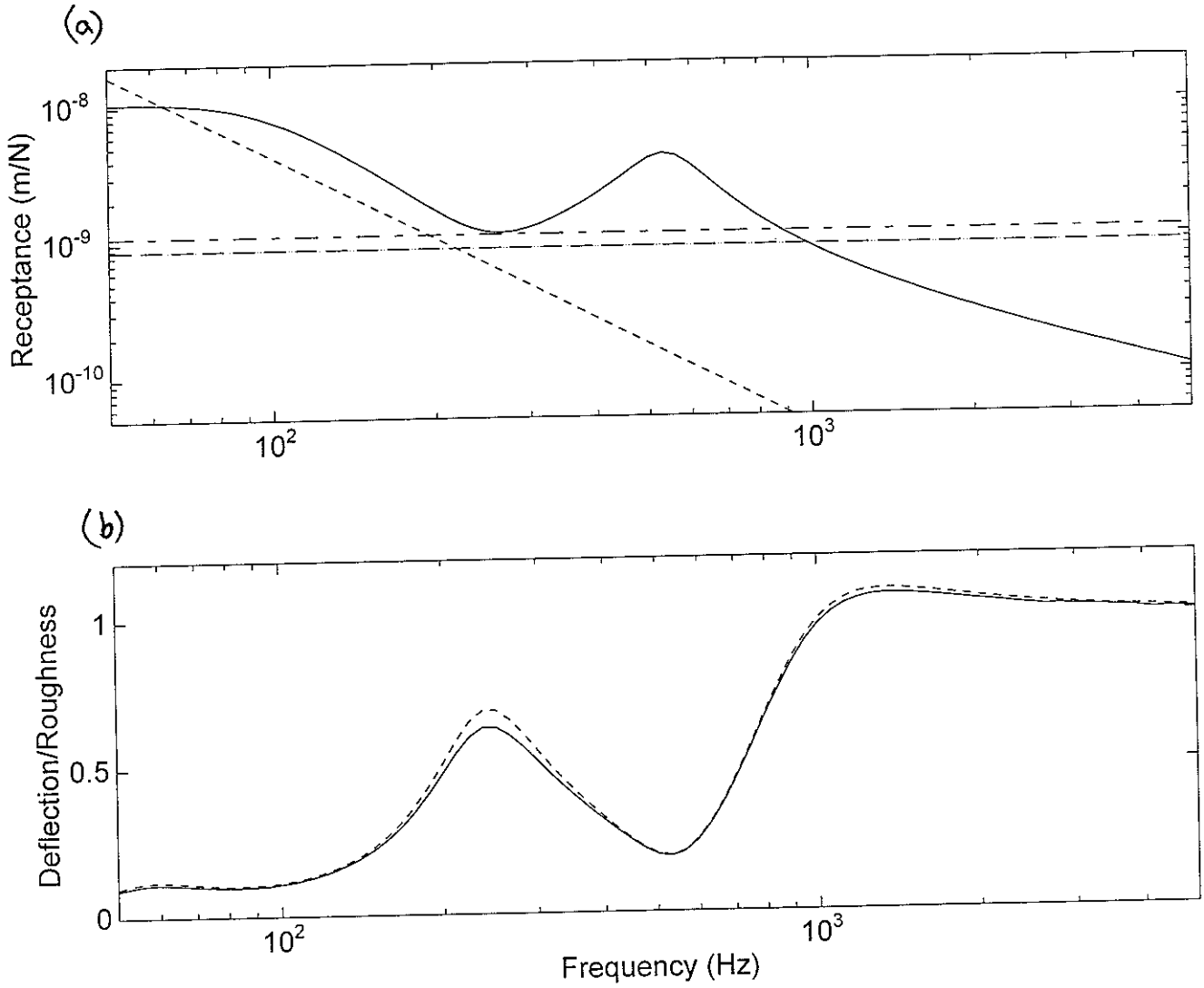

Figure 10. (a) Receptances of the wheel, track and the equivalent tangent contact stiffness. — rail receptance, ····· wheel receptance, - - - receptance of tangent stiffness under static load 50 kN, ----- receptance of tangent stiffness under static load 25 kN. (b) Ratio of the amplitude of the dynamic contact deflection to the roughness input, the static load $W = 50$ kN. — from the linear contact, ····· from the non-linear contact.

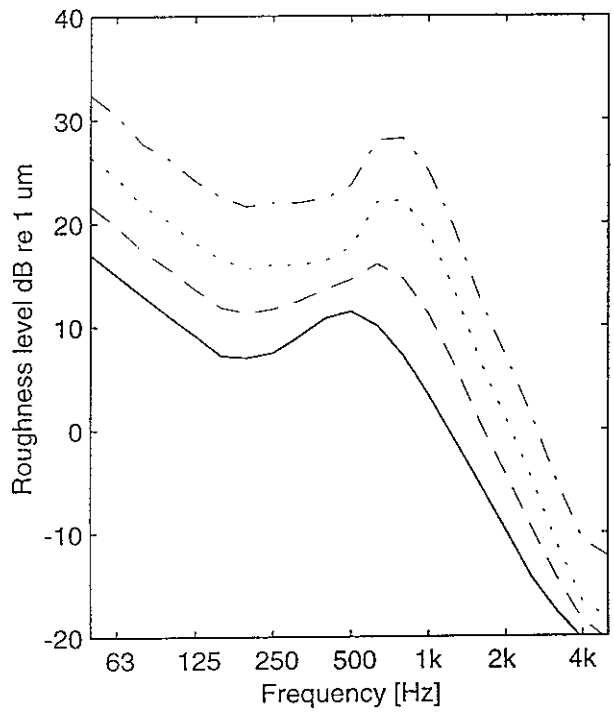

Figure 11. Assumed one-third octave band roughness spectra. — cast-iron block braked wheel on good track at 100 km/h, - - - intermediate roughness, ····· corrugated rail roughness at 140 km/h, - · - · extreme roughness.

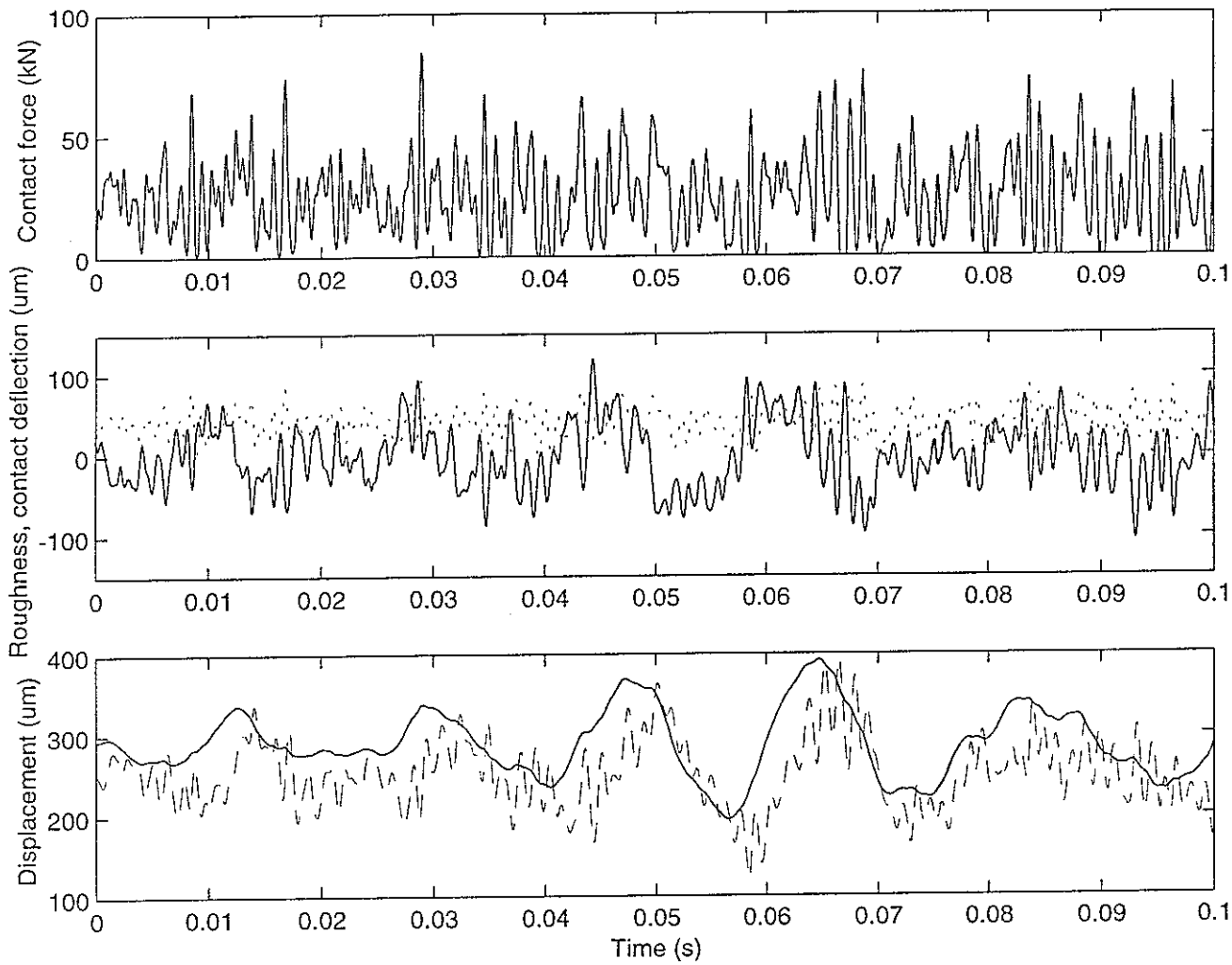

Figure 12. The non-linear wheel/rail contact force, broad band random roughness input (from corrugated track, spectrum from Figure 11) and the wheel and rail displacements, the static load $W = 25$ kN. (a) contact force, (b) — roughness input, ····· contact deflection, (c) — wheel displacement, - - - rail displacement.

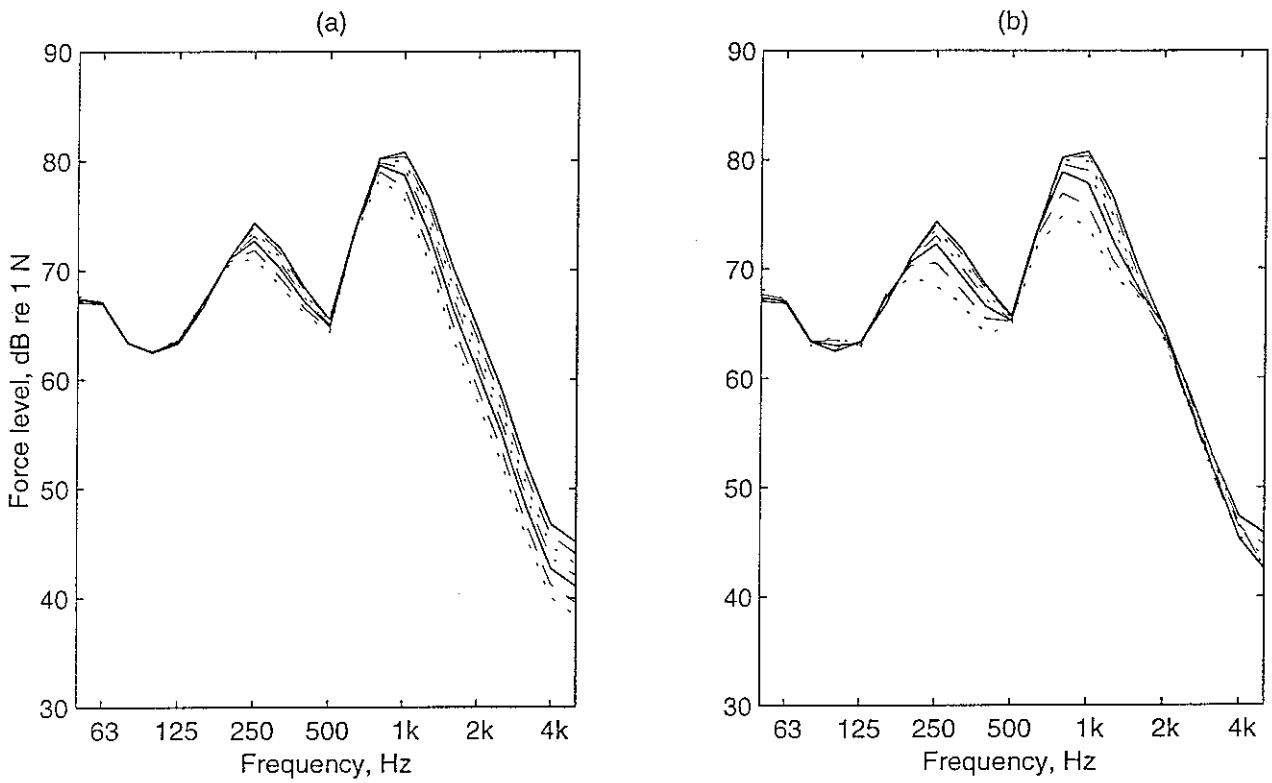

Figure 13. One-third octave band spectra of the wheel/rail contact force for corrugated track roughness, (a) from the linear model, (b) from the non-linear model. From bottom to top, static load W = 10, 15, 25, 35, 50, 70, 100 kN.

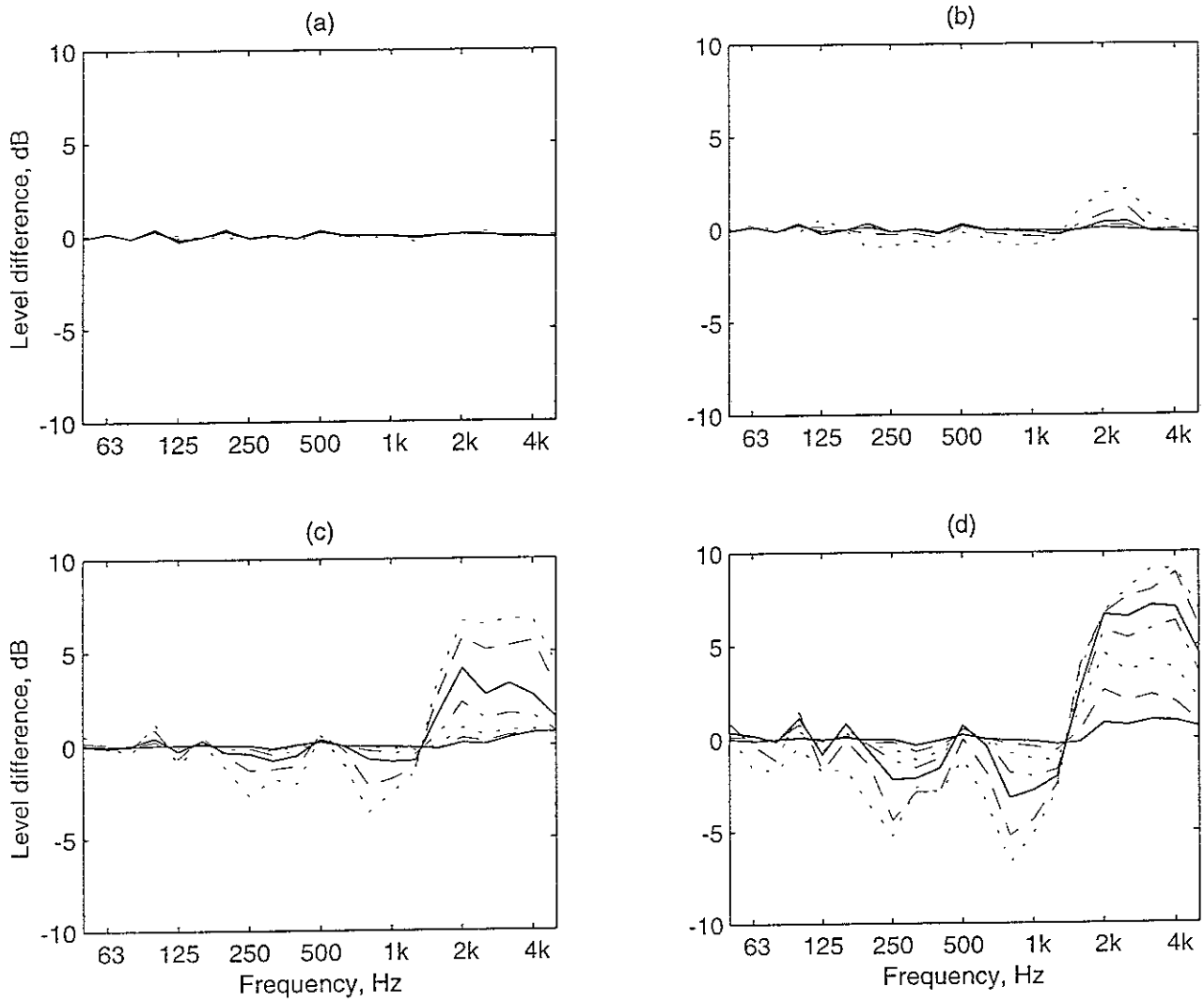

Figure 14. Difference in one-third octave band spectra of the wheel/rail contact force from the non-linear model compared to the linear model. From largest deviations to smallest, static load W = 10, 15, 25, 35, 50, 70, 100 kN. (a) tread-braked wheel roughness at 100 km/h, (b) intermediate roughness, (c) corrugated rail roughness at 140 km/h, (d) extreme roughness (amplitude doubled from (c)).

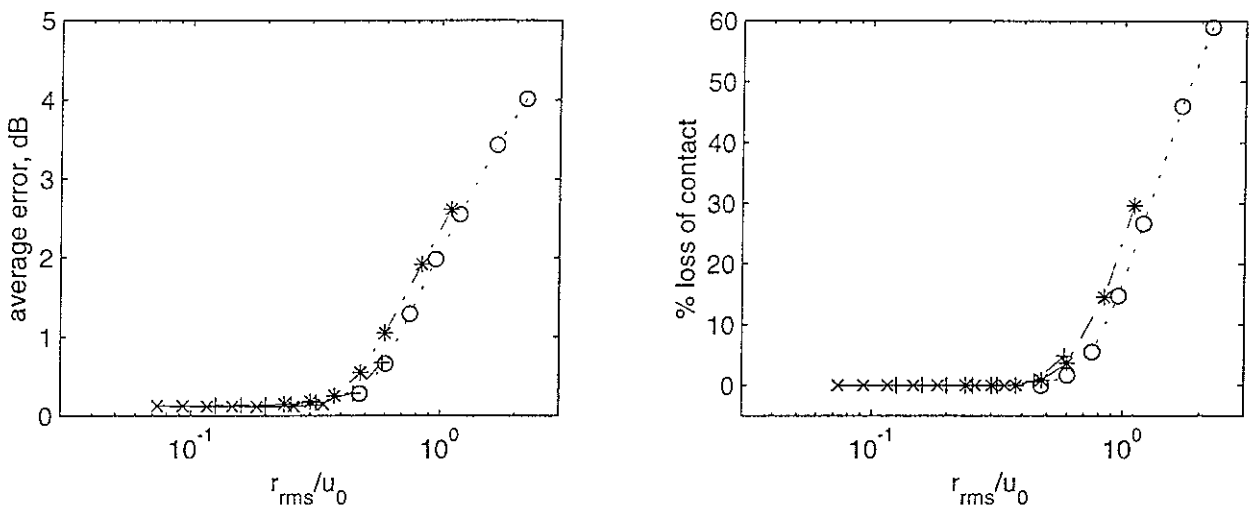

Figure 15. (a) Average difference in one-third octave band spectra of the wheel/rail contact force from the non-linear model compared to the linear model plotted against ratio of r.m.s. roughness amplitude to static contact deflection. (b) percentage of time that contact is fully unloaded plotted against ratio of r.m.s. roughness amplitude to static contact deflection. ×: tread-braked wheel roughness at 100 km/h, +: intermediate roughness, *: corrugated rail roughness at 140 km/h, o: extreme roughness.